Journal of Hazardous Materials 470 (2024) 134088

Contents lists available at ScienceDirect

Journal of Hazardous Materials

journal homepage: www.elsevier.com/locate/jhazmat

Elucidation of arsenic detoxification mechanism in *Marchantia polymorpha*: The role of ACR3

Mingai Li [a,b,*], Aurélien Boisson-Dernier [c], Daniela Bertoldi [d], Francisco Ardini [e], Roberto Larcher [d], Marco Grotti [e], Claudio Varotto [a,b,*]

[a] Biodiversity, Ecology and Environment Area, Research and Innovation Centre, Fondazione Edmund Mach, via Mach 1, San Michele all'Adige, 38098 Trento, Italy
[b] NBFC, National Biodiversity Future Center, Palermo 90133, Italy
[c] Université Côte d'Azur, INRAE, CNRS, Institut Sophia Agrobiotech, 400 Route des Chappes, BP167, 06903 Sophia Antipolis Cedex, France
[d] Department of Food and Transformation, Technology Transfer Centre of Fondazione Edmund Mach, E. Mach 1, San Michele all'Adige, 38098 TN, Italy
[e] Department of Chemistry and Industrial Chemistry, University of Genoa, Via Dodecaneso 31, Genoa, Italy

HIGHLIGHTS

- Knockout mutants of *Marchantia polymorpha* arsenite transporter Mp*ACR3* were obtained.
- MpACR3 plays a pivotal role in arsenic (As) detoxification in *M. polymorpha*.
- MpACR3 regulates the amount of As in the plant possibly by extrusion to the apoplast.
- The mutants are more sensitive and over-expressors more tolerant to As than WT Cam2.
- These *M. polymorpha* mutants constitute a highly specific bioindicator for As in water.

GRAPHICAL ABSTRACT

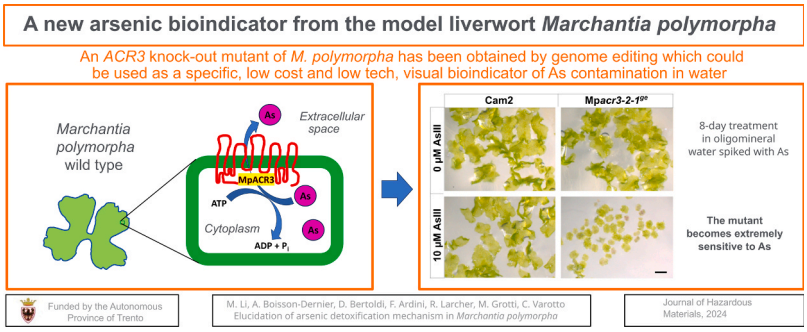

ARTICLE INFO

Keywords:
Arsenic extrusion
Transporter
Drinking water
Bioindicator

ABSTRACT

The arsenic-specific ACR3 transporter plays pivotal roles in As detoxification in yeast and a group of ancient tracheophytes, the ferns. Despite putative *ACR3* genes being present in the genomes of bryophytes, whether they have the same relevance also in this lineage is currently unknown. In this study, we characterized the Mp*ACR3* gene from the bryophyte *Marchantia polymorpha* L. through a multiplicity of functional approaches ranging from phylogenetic reconstruction, expression analysis, loss- and gain-of-function as well as genetic complementation with an Mp*ACR3* gene tagged with a fluorescent protein. Genetic complementation demonstrates that Mp*ACR3* plays a pivotal role in As tolerance in *M. polymorpha*, with loss-of-function Mp*acr3* mutants being hypersensitive and Mp*ACR3* overexpressors more tolerant to As. Additionally, MpACR3 activity regulates intracellular As concentration, affects its speciation and controls the levels of intracellular oxidative stress. The MpACR3::3x-Citrine appears to localize at the plasma membrane and possibly in other endomembrane systems. Taken together, these results demonstrate the pivotal function of ACR3 detoxification in both sister lineages of land plants, indicating that it was present in the common ancestor to all embryophytes. We propose that Mp*acr3*

* Corresponding authors at: Biodiversity, Ecology and Environment Area, Research and Innovation Centre, Fondazione Edmund Mach, via Mach 1, San Michele all'Adige, 38098 Trento, Italy.
E-mail addresses: mingai.li@fmach.it (M. Li), claudio.varotto@fmach.it (C. Varotto).

https://doi.org/10.1016/j.jhazmat.2024.134088
Received 18 January 2024; Received in revised form 28 February 2024; Accepted 18 March 2024
Available online 19 March 2024

mutants could be used in developing countries as low-cost and low-technology visual bioindicators to detect As pollution in water.

1. Introduction

Arsenic (As) ranks in the first position of the 2022 US Agency for Toxic Substances and Disease Registry (ATSDR)'s Substance Priority List (https://www.atsdr.cdc.gov/spl/index.html#2022spl), making it the most significant potential threat to human health in the United States according to a weighted combination of frequency, toxicity, and potential for human exposure. Inorganic As is a ubiquitous Group 1 carcinogen (https://monographs.iarc.who.int/wp-content/uploads/2018/06/mono100C.pdf; https://cfpub.epa.gov/ncea/iris/iris_documents/documents/subst/0278_summary.pdf) in environments worldwide, and human exposure through intake of contaminated water or food (especially rice) is a major health concern worldwide [21,51,52]. Often listed, although somehow inappropriately from a chemical point of view, among the toxic metal elements [56], in addition to causing various types of cancer, above defined thresholds As can also increase the risk of cardiovascular [50] and other types of diseases [18]. It has been estimated that between 94 and 220 million people worldwide are exposed to potentially toxic concentrations of As just from naturally contaminated (geogenic) ground water [54], without counting sources from anthropic sources like mining, metallurgy, energy production, agriculture and various types of industries [4,60].

Also plants suffer from As toxicity and therefore they evolved different systems of As detoxification and, in very few cases, even hyperaccumulation [3]. In the current oxygen-rich atmosphere the prevalent form of As present in soils is arsenate (AsV), although in anoxic conditions significant amounts of soil inorganic arsenic can be present as arsenite (AsIII; [53]). Under oxygenic conditions, arsenate is imported from soil into the plant cell mainly through phosphate transporters [23], and the majority of AsV is quickly reduced to AsIII by the As-specific high arsenic content (HAC1) reductase [11]. In angiosperms, cytosolic AsIII is mainly complexed with phytochelatins, low molecular weight polypeptides synthesized non-ribosomally by the enzyme phytochelatin synthase (PCS; [29]), and transported for detoxification into the vacuole [64].

In contrast, gymnosperms and all earlier evolved lineages of embryophytes (ferns and horsetails, lycopods and bryophytes), seem to share together with fungi and some bacteria an additional detoxification system missing in angiosperms that relies on the active extrusion of AsIII from the cell mediated by the arsenic compounds resistance 3 (ACR3) protein, a membrane H^+/AsIII antiporter [33,47,70,8]. While the substrate specificity, kinetic constants and mechanism of action have been determined in detail for the *Saccharomyces cerevisiae* Meyen ex E.C. Hansen ACR3 (also called ARR3) transporter [47,49], until now the only *ACR3* genes characterized from land plants are those from the As hyperaccumulator fern *Pteris vittata* compl., the first one to have been discovered and one of the highest hyperaccumulators to date [45,71]. Early functional studies showed that down-regulation of *PvACR3* expression, but not of its paralogue *PvACR3;1*, by RNAi in *P. vittata* gametophytes causes a dramatic increase of the sensitivity to As, providing the first functional hints of specialization between the different copies [33].

P. vittata is a species complex characterized by five ploidy levels, namely diploid, triploid, tetraploid, pentaploid and hexaploid [12], with tetraploid and pentaploid cytotypes being dominant in India [48]. Until now five *PvACR3* copies have been identified and functionally validated [13,43,65], but several other paralogs may exists [65] knowing the polyploidy of the individuals used for analysis in previous studies. Most importantly, such genetic redundancy may indeed be one of the factors that likely contributed to the evolution of As hyperaccumulation in *P. vittata*, allowing the functional specialization of the different copies both in terms of subcellular localization and tissue-specific expression to result in a highly efficient transfer from the roots to the fronds where As is stored in high quantities in the vacuoles of trichomes [43,71]. In support to this model, two of the PvACR3 transporters (PvACR3 and PvACR3;2) are localized to the plasma membrane and have been implicated in root to frond As mobilization, while the other three (PvACR3;1, PvACR3;3 and PvACR3;4) reside in the tonoplast membrane where they are thought to contribute to As detoxification by sequestering it into the vacuole [13,14,43,65].

Several studies have demonstrated how overexpression of different *ACR3* genes from *P. vittata* in heterologous systems like *Arabidopsis thaliana* (L.) Heynh., *Nicotiana tabacum* L. and *S. cerevisiae* are able to increase As tolerance (e.g. Chen et al., [14,15,68]). Worth noting, the pathway of As detoxification mediated by phytochelatin complexation and sequestration into the vacuole seems to play a marginal role in As tolerance in *P. vittata* [72]. Whether this is the case also in the other groups of land plants possessing both the phytochelatin-based and the ACR3-based detoxification pathways is currently unknown, as to date *P. vittata* is the only species for which the relative contribution of the phytochelatin- and the ACR3-mediated As detoxification pathways has been elucidated.

Ferns like *P. vittata* belong to the tracheophytes, or vascular plants, which are the largest of the two monophyletic sister clades constituting the lineage of land plants (also called embryophytes; [20]). The other clade of embryophytes, the bryophytes, is a group of diminutive, non-vascular plants encompassing mosses, liverworts and hornworts [61]. By contrast to tracheophytes, bryophytes are characterized by a simpler body plan lacking true leaves, stems, roots and fully differentiated vascular tissues and their life cycle is dominated by a haploid, multicellular phase constituted by free-living and long-lived gametophytes [24]. Besides being the second most numerous group of land plants, bryophytes are evolutionarily relevant, as their comparison to tracheophytes can provide precious insights into the evolution of specific traits along the green lineage and determine whether they were present in the common ancestor to all land plants [28]. Among bryophytes, liverworts are a species-rich monophyletic clade with the majority of species having small genomes with low levels of genetic redundancy due to the rare occurrence of whole genome duplications during their evolutionary history [41]. The most important model species among liverworts is by far the thallose liverwort *Marchantia polymorpha*, owing to its short life cycle, easy propagation with both sexual and asexual systems, high quality genome assembly as well as a complete set of functional-genomics tools [9].

Recently, we started developing *M. polymorpha* as a model organism to dissect from an evolutionary perspective the mechanisms of toxic metal and metalloid tolerance in land plants [22,38,39,5,6]. Following the obtainment of genome-edited knockout *M. polymorpha* lines with complete loss of function of its single copy *PCS* gene, it became apparent that in *M. polymorpha* the phytochelatin-mediated pathway of As detoxification is either secondary or redundant to another, as yet not functionally characterized, As detoxification pathway [39]. Owing to the presence of a single-copy ortholog of *ACR3* in the genome of *M. polymorpha*, we speculated that Mp*ACR3* could play a major role in As detoxification in this and other bryophytes species [39].

The aim of the present study was to functionally test this hypothesis through a combination of genetic, physiological and cell biology approaches. In detail, we wanted to answer the following open questions: 1) Is the ACR3-mediated pathway a major mechanism of As detoxification in bryophytes? 2) If so, is the trait ancestral to all land plants? 3) What are the similarities and differences in the As detoxification mechanism existing in *P. vittata*, whose genome bears multiple *ACR3*

paralogs, and in *M. polymorpha*, having a single *ACR3* gene?

2. Materials and methods

2.1. Plant materials, growing conditions and arsenic treatments

The liverwort *Marchantia polymorpha* L. Cam2 (UK Cambridge-2 wild type) female gametophytes, two independent Mp*acr3* knockout mutants (Mp*acr3–1-5*^{ge} and Mp*acr3–2-1*^{ge}) in *M. polymorpha*, and two independent transgenic lines overexpressing Mp*ACR3* (Mp*ACR3-ox-9* and Mp*ACR3-ox-10*) in *M. polymorpha* were used in this study. *M. polymorpha* was generally propagated in a half strength Murashige and Skoog (MS) medium supplemented with 1% sucrose and 1% phytoagar under a light intensity of 60 μmol m^{-2} s^{-1} with photoperiod of 16 h light and 8 h dark at 21 °C in a growth chamber.

For growth assay of Cam2 wild-type plants and Mp*acr3* knockout mutants in oligomineral water (100 μM $(NH_4)_2HPO_4$, 200 μM $MgSO_4$, 280 μM $Ca(NO_3)_2$, 600 μM KNO_3, 5 μM Fe-HBED, pH 7.0; [67]), around 40 gemmae of different genotypes were transferred into 60 mm petri dish (Sarstedt, Germany) containing fresh oligomineral water or with addition of 10 μM AsIII/AsV and covered with lids, respectively. The plants were grown for eight days under the standard long-day photoperiod as mentioned above and five replicates in each condition for each genotype were used.

For biomass analyses upon heavy metal treatments in *M. polymorpha*, fresh gemmae from wild-type Cam2, two knockout mutants (Mp*acr3–1-5*^{ge} and Mp*acr3–2-1*^{ge}) and two overexpression lines (Mp*ACR3-ox-9* and Mp*ACR3-ox-10*) were grown in 1/10 hydroponic solid medium as previously described [67] for 10 days (Mp*acr3* knockout mutants and Mp*ACR3* overexpressing lines) and then either grown without any arsenic addition or exposed to different concentrations of AsIII/AsV for two weeks before measurement. The MpACR3::3xCitrine

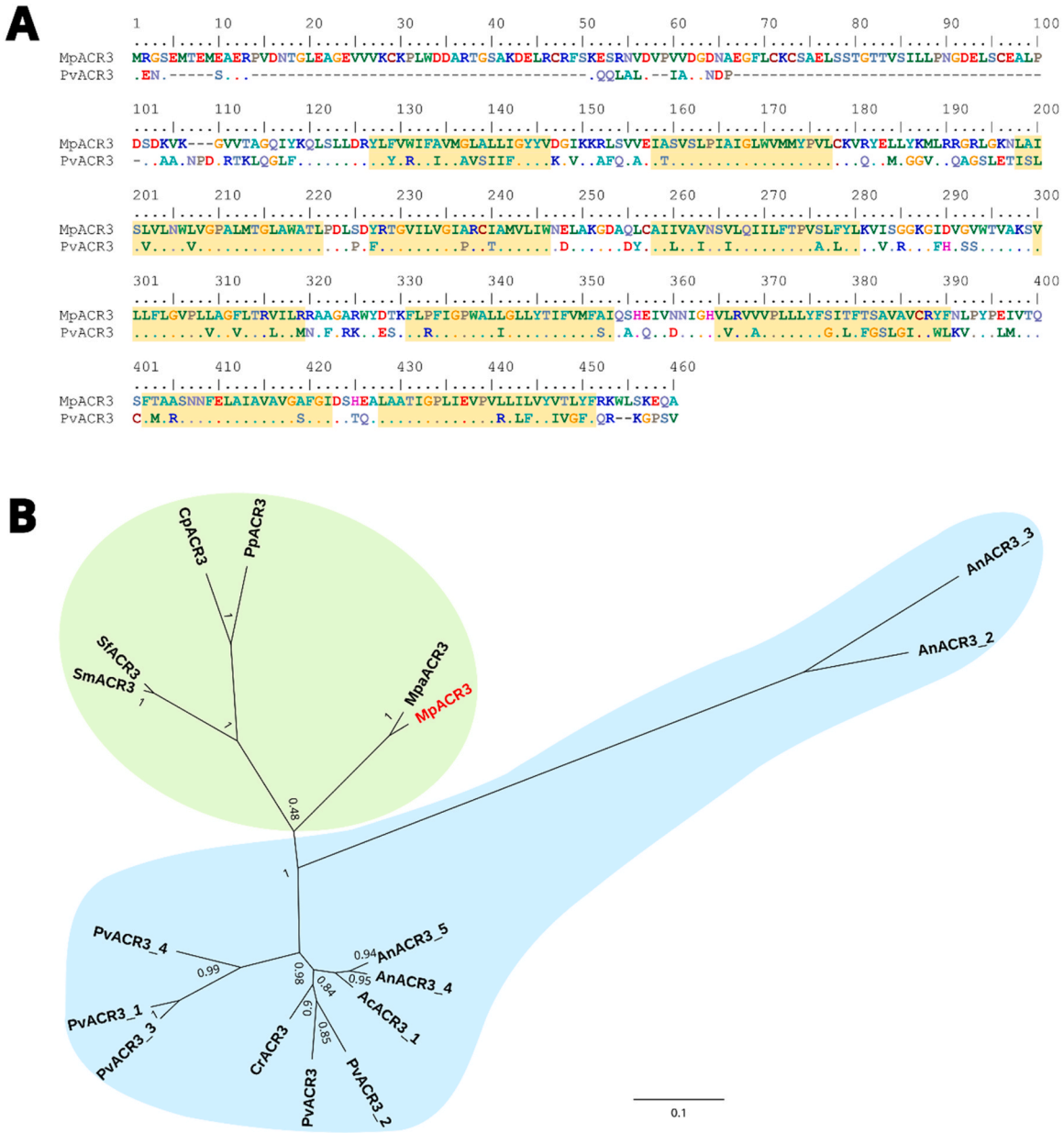

Fig. 1. Protein alignment and phylogenetic tree of MpACR3. (A) Protein alignment of MpACR3 and PvACR3. Dots represent identical amino acids. Dashes are gaps in the alignment. Predicted transmembrane regions are highlighted in light yellow. (B) ML phylogenetic tree of different ACR3 proteins from selected ferns (light blue background) and bryophytes (light green) species. The label of MpACR3 is highlighted in red. Numbers close to the branches are SH-like branch supports. The protein accession numbers and corresponding species used to construct the phylogenetic tree are listed in Supplementary Table S1.

complementation lines of the Mp*acr3–1-5*^{ge} mutant (see below) were grown for 16 days in the same medium and then exposed to different concentrations of AsIII (0 μM, 200 μM and 400 μM) for one week before measurement. The biomass analyses were conducted with at least six biological replicates.

2.2. Phylogenetic reconstruction

The MpACR3 protein homolog from *M. polymorpha* was identified by blastp [2] homology searches using *P. vittata* PvACR3 as a query against the whole *M. polymorpha* proteome with an e-value threshold of 10^{-5}. The proteins were aligned with Clustalw in Bioedit and the transmembrane spanning region was identified from the alignment based on *Saccharomyces cerevisiae* ScACR3 annotation (UNIPROT accession Q06598). An analogous strategy was used to identify the protein homologs used for phylogenetic analyses by limiting the searches to bryophytes and ferns in both Phytozome 13 [25] and the GenBank nr protein databases [7] and eliminating redundant hits. PvACR3;4 was mined by tblastn in the transcriptome of *P. vittata* [65]. The selected proteins were aligned with MAFFT v. 7 [35] using default parameters. The resulting alignments were visually inspected and low-quality alignment regions removed with the help of Gblocks v. 0.91b [66] using the following parameters: minimum number of sequences for a conserved position: 9, minimum number of sequences for a flanking position: 14, maximum number of contiguous nonconserved positions: 8, minimum length of a block: 5, allowed gap positions: 50%, use similarity matrices: Yes. The refined alignment was subjected to maximum likelihood phylogenetic reconstruction using PhyML v. 3.0 with default parameters [27]. Protein accession numbers for all taxa in Fig. 1B are listed in Supplementary Table S1.

2.3. Total RNA extraction, cDNA synthesis and RT-PCR analyses

Around 100 mg of collected plant material was used for total RNA extraction using Spectrum Plant Total RNA Kit (Sigma-Aldrich®), and the quality evaluation of the extracted total RNA and cDNA synthesis were carried out as previously described [55]. Semi-quantitative RT-PCR for different organs of *M. polymorpha* and overexpressing Mp*ACR3* transgenic lines was carried out in a thermal cycler using Taq DNA polymerase (Sigma-Aldrich®) with the primers listed in Supplementary Table S2 and Mp*ACT* gene as an internal reference.

To analyze the transcript response of Mp*ACR3* to AsIII/AsV treatment, 10-day-old Cam2 plants were exposed to either 60 μM of AsIII or 200 μM of AsV, and plant materials were harvested at 0 h, 1 h, 3 h, 6 h, 12 h and 24 h for RNA extraction. Quantitative real time-PCR (qRT-PCR) was carried out with Platinum SYBR Green qPCR SuperMix-UDG (Invitrogen) in a Bio-Rad C1000 Thermal Cycler detection system using Mp*ACT* and Mp*APT* as reference genes in *M. polymorpha* [58]. The qRT-PCR results were calculated from at least three technical and three biological replicates per sample. The relative transcription level of each gene was calculated with the $2^{-\Delta\Delta CT}$ method. The primers used for this analysis are listed in Supplementary Table S2.

2.4. Plasmid constructs and plant transformation

The CRISPR/cas9 plasmid constructs were generated according to former description [39] using the oligonucleotides listed in Supplementary Table S2.

For overexpression of Mp*ACR3* in *M. polymorpha*, Mp*ACR3* coding sequence was amplified from wild-type Cam2 cDNA synthesized as mentioned above using primers MpACR3_For and MpACR3_Rev with Phusion High Fidelity DNA Polymerase (Thermo Scientific), cloned into pENTR/D-TOPO vector (Invitrogen) and recombined into the destination vector pMpGWB103 [34] with LR clonase II Enzyme Mix (Invitrogen).

For the Mp*ACR3* complementation construct in the Mp*acr3* mutant background of *M. polymorpha*, the entire genomic locus from the position − 3392 bp upstream of the start codon till the codon immediately before the stop codon was amplified from Cam2 genomic DNA with the primers listed in Supplementary Table S2 using Q5 High-Fidelity DNA Polymerase (New England Biolabs), cloned into the entry vector and recombined into pMpGWB323 vector as mentioned above.

All constructs were first transformed into *Agrobacterium tumefaciens* strain GV3101-pMP90RK by electroporation and further into *M. polymorpha* as previously described [36]. T1 transgenic plants growing on half-strength solid Gamborg B5 medium containing either 10 mg/l hygromycin used for the selection of knockout mutants and overexpression lines or 0.5 μM chlorsulfuron for complementation lines were selected, and a single gemma derived from each T1 line was grown to generate gemmae which were used for all downstream work.

All constructs described above were validated by sequencing with a 96-capillary 3730xl DNA Analyzer (Thermo Fisher Scientific).

2.5. Genotyping of transformants

Genomic DNA was extracted from thalli harboring the CRISPR/Cas9, Mp*ACR3* overexpression and complementation constructs with the CTAB method [1] and used for PCR amplification. The PCR reactions were performed using the primers listed in Supplementary Table S2 and Phusion High-Fidelity DNA polymerase (Thermo Fisher Scientific). The PCR amplicons of the target gene were purified and sequenced as previously described [39].

2.6. Lipid peroxidation analyses

Ten-day-old plants of different *M. polymorpha* genotypes growing in solid 1/10 hydroponic medium were transferred into fresh medium supplemented without or with 75 μM AsIII for Mp*acr3* knockout mutants or 1600 μM AsIII for Mp*ACR3* overexpression lines. Around 100 mg of plant materials were collected in liquid nitrogen at days 3 and 5 after AsIII exposure and stored at − 80 °C. Lipid peroxidation of the collected samples was assessed by malondialdehyde (MDA) production using the thiobarbituric acid (TBA) method [31].

2.7. Total Arsenic assay

For total arsenic analyses 10-day-old *M. polymorpha* plants from each genotype were grown in solid 1/10 hydroponic medium as above and treated without or with different concentrations of Arsenic (25 μM AsIII and 85 μM AsV for knockout mutants, and 600 μM AsIII and 900 μM AsV for overexpression lines) in a fresh medium for 72 hr. Afterwards, the plant materials were harvested, immersed in ice-cold solution containing 1 mM K_2HPO_4, 0.5 mM $Ca(NO_3)_2$ and 5 mM MES (pH 6.0) for 10 min, blotted dry and frozen in liquid nitrogen. The frozen plant materials were lyophilized and acid digested with ultrapure nitric acid as previously described [39]. Elemental quantities in the samples were determined with an inductively coupled plasma mass spectrometer (ICP-MS, Agilent 7800, Agilent Technologies, Tokyo, Japan) equipped with an octopole collision cell (He mode, 5 mL/min) for polyatomic interference reduction.

2.8. Arsenic speciation analyses

For Arsenic speciation analyses 15-day-old *M. polymorpha* plants were transferred into fresh liquid 1/10 hydroponic medium supplemented with 10 μM AsV and kept for 24 h. The plant materials were collected, soaked, and lyophilized as mentioned above and stored in the dark at room temperature. The liquid medium was also collected and stored at − 20 °C till use.

Total arsenic concentrations in the extracts and solutions were determined by ICP-MS (Elan DRCII by Perkin-Elmer, Waltham, MA, USA), after 10-fold or 100-fold dilution with ultrapure water, using the

external calibration with standard solutions in the 0–10 μg/L range. Procedural blanks were concomitantly prepared and analyzed.

To quantify As species in the plants, a portion (ca 25–60 mg weighed with a precision of ± 0.1 mg) of each freeze-dried sample was transferred into a 15-mL polypropylene graduated conical test tube (VWR International) and treated with 5 mL of methanol/water (1 +4 v/v) extraction solution, shaking top over bottom overnight at ambient temperature. Then, the extracts were filtered through 0.45 μm regenerated cellulose filters (Sartorius; Goettingen, Germany) and analyzed by anion-exchange HPLC-ICP-MS. Chromatographic separations were performed on a PRP-X100 column (250 ×4.1 mm, 10 μm particles; Hamilton, Reno, USA) at 40 °C with a mobile phase of 20 mM aqueous ammonium dihydrogen phosphate of pH 6.0 (adjusted with aqueous ammonia), at a flow rate of 1.0 mL min^{-1}. Methanol was added to the mobile phase (2 +98 v/v) to enhance the signal response. The injection volume was 20 μL. Arsenite and arsenate were identified by retention time matching and quantified by external calibration using standard solutions in the 0–100 μg/L range.

2.9. Confocal laser scanning microscopy of gemmae expressing MpACR3::3xCitrine

Young gemmae from 3 independent complemented lines expressing MpACR3::3xCitrine (this study) were incubated in 12-well-plates with 2 mL of 1/2 strength Gamborg liquid medium per well. Gemmae were left to grow for 24 h before being sandwiched between a slide and a coverslip spaced with a bit of parafilm containing fresh 1/2 strength Gamborg liquid medium with or without propidium iodide (PI; 5 mg/L). Confocal laser scanning microscopy was performed using an inverted Zeiss LSM 880 microscope, equipped with Argon ion and HeNe lasers as excitation sources. Images were taken using a Plan-Apochromat 20x/0.8 M27 objective at a resolution of 1024 × 1024 pixels, a pinhole size of 1 AU, and a scan speed of 400–700 Hz using HyD hybrid detectors. Citrine, PI, and Chlorophyll were excited at 514 nm, and their emissions were collected between 516–556 nm, 590–620 nm and 634–704 nm, respectively. Confocal images were processed using ImageJ/FIJI [59]. Data manipulation included maximum or best focus projections from Z-stacks (≤20 frames, 1 μm slice intervals), Gaussian blur filtering, as well as generation of composite images from separate individual channels.

2.10. Statistical analyses

Statistical significance among mean values for the different measurements was assessed based on Student's *t*-tests carried out for each measurement versus the respective control (untreated control, or wild type genotype, depending on the experiment). For numbers of *t*-tests higher than 4, the false discovery rate (fdr) correction for multiple testing was applied and the corrected p-value reported. The number of stars, unless otherwise specified, represent the level of statistical significance of each Student's *t*-test according to the following coding conventions: * : $p <= 0.05$; **: $p <= 0.01$; *** : $p <= 0.001$; ****: $p <= 0.0001$. All experiments were performed with at least $n = 3$ biological replicates.

3. Results

3.1. MpACR3 is the only orthologue of PvACR3 in M. polymorpha and its ubiquitous transcription is upregulated by arsenic treatment

It has been demonstrated that the genes belonging to the *PvACR3* family play an essential role in As detoxification/hyperaccumulation in the fern *P. vittata*. To determine whether any orthologue(s) of *PvACR3* exist in *M. polymorpha*, we carried out a homology search of the PvACR3 protein sequence against the full set of proteins of the sequenced *M. polymorpha* genome [10]. A single-copy putative ACR3 orthologue was identified in *M. polymorpha* (accession number Mp5g06690.1). The full-length cDNA of the Mp*ACR3* gene encodes a predicted polypeptide of 457 amino acids, sharing 70.3% sequence identity with PvACR3 in the region between residues 114 to 450 (Fig. 1A). A long, low homology N-terminal extension constitutes the major difference from PvPCR3 (Fig. 1A). Phylogenetic reconstruction with selected ACR3 proteins from fern and bryophyte species with fully sequenced genomes in the Phytozome 13.0 database, confirmed that MpACR3 is a *bone-fide* ACR3 As transporter: Consistently with the known phylogenetic relationships among land plants, MpACR3 clusters with the orthologues from the other bryophytes analyzed (light green shading in Fig. 1B), while the ACR3 proteins from ferns, including those from *P. vittata*, form a separate cluster (light blue shading in Fig. 1B).

To understand the functional relevance of Mp*ACR3*, first we evaluated its expression pattern in different organs from plants growing in standard long-day conditions using semi-quantitative RT-PCR. This analysis indicated that Mp*ACR3* is expressed in all different organs tested, and the stronger expression level was detected in two-week-old plantlets (Fig. 2A). In addition, to evaluate whether the transcriptional level of Mp*ACR3* is regulated by external As exposure, ten-day-old Cam2 wild type plants treated either without or with 60 μM AsIII/200 μM AsV were harvested at different time points and used for real-time qRT-PCR analysis. Two reference genes (Mp*ACT* and Mp*APT*) were used for normalization [38]. The expression of Mp*ACR3* was upregulated by both oxidation states of As applied, although the intensity of the induction varied due to the different concentrations of AsIII and AsV used for treatment (Figs. 2B and 2C).

3.2. MpACR3 loss-of-function mutants of M. polymorpha are hypersensitive to both arsenite and arsenate

To dissect in detail the functional contribution of MpACR3 to As detoxification in *M. polymorpha*, we designed sgRNAs for targeting by CRISPR-CAS9 two independent regions of the Mp*ACR3* gene (Fig. S1A), one at the beginning of the first exon, while the second towards the end of the second exon. Having the genomic targets different sequences, this strategy virtually eliminates the risk of false positive phenotypes, as the groups of the (few) potentially off-target mutations do not overlap. Among the multiple transgenic lines obtained with each construct, we chose Mp*acr3–1-5*^{ge} and Mp*acr3–2-1*^{ge} for target 1 and 2, respectively. Mp*acr3–1-5*^{ge} causes a 2-bp deletion after only 16 codons from the protein start codon and a premature stop codon after 22 residues. Mp*acr3–2-1*^{ge} results in a 2 bp insertion disrupting the protein translation frame after the 99th residue of the protein and a premature stop codon after 131 amino acids (Fig. S1B). When no As was present in the growth medium, no differences between Cam2 and the Mp*acr3* mutants could be detected (Figs. 3A and 3B). When challenged with two different concentrations of either AsIII or AsV in the culture medium, the phenotype of both mutants was identical, and it was characterized by a severe reduction of growth as measured by fresh weight and at the higher concentrations of both As species by chlorosis and death despite no significant alteration of Cam2 WT growth or vitality in the same conditions (Figs. 3A and 3B). Thus, loss-of-function of Mp*acr3* confers hypersensitivity to As in *M. polymorpha* and MpACR3 positively regulates As tolerance.

3.3. MpACR3 gain-of-function lines of M. polymorpha are tolerant to both arsenite and arsenate

Stable overexpression of Mp*ACR3* under the control of the strong Mp*EF1α* promoter was carried out to test whether the gain of function of the gene could improve the tolerance of Cam2 WT to As. Among the 13 independent transgenic *M. polymorpha* lines obtained, we chose the two with the highest expression of the transgene as assessed by semi-quantitative RT-PCR (Mp*ACR3-ox-9* and Mp*ACR3-ox-10*; Fig. S2). In the absence of As in the growth medium no significant differences in

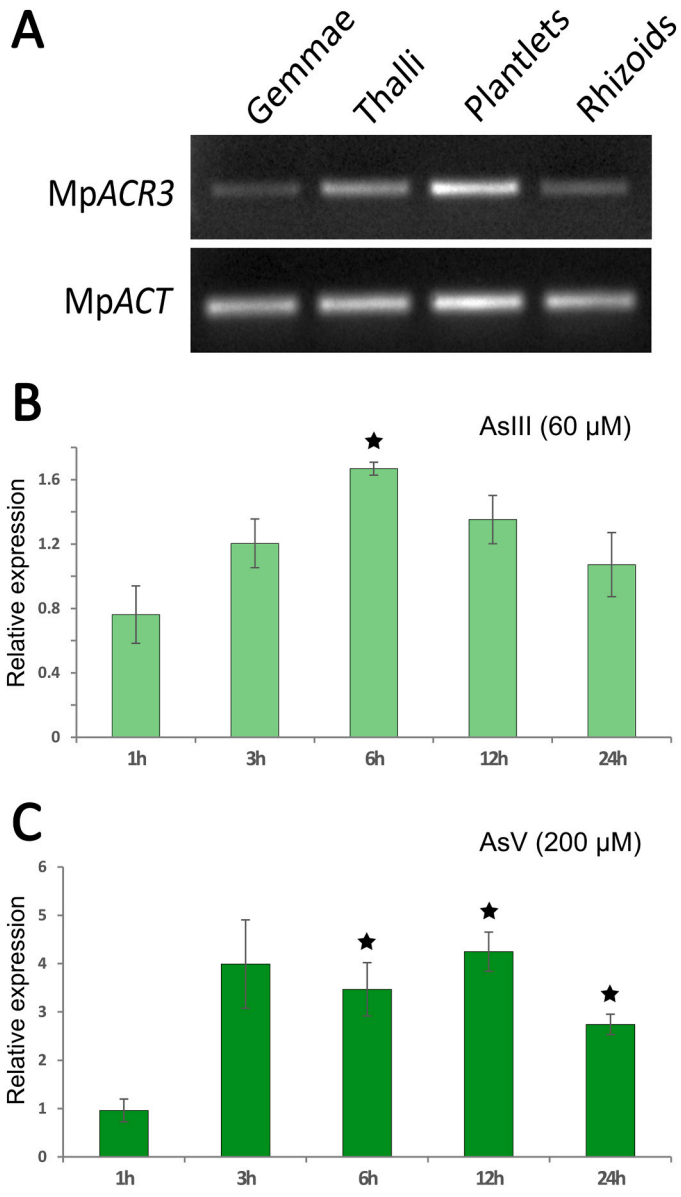

Fig. 2. Expression patterns of Mp*ACR3* in different organs/tissues and inducibility by As in *M. polymorpha* Cam2. (A) Semi-quantitative RT-PCR of Mp*ACR3* expression in different organs/tissues. (B) Time course of Mp*ACR3* transcription levels quantified by real-time qRT-PCR in response to AsIII or AsV treatments. Values for each time point are averages and the error bars are standard deviations of three biological replicates (n = 3). Stars indicate significant differences compared to time 0 h (untreated control) according to Student's *t*-test followed by false discovery rate (fdr) multiple test correction ($P < 0.05$).

fresh weight could be detected between overexpressing lines and Cam2 gametophytes (Figs. 4A and 4B). Both Mp*ACR3* overexpressing lines, on the other hand, grew consistently faster and accumulated more biomass than Cam2 gametophytes when different concentrations of either AsIII or AsV were added to the growth medium (Figs. 4A and 4B), demonstrating that the MpACR3 gain-of-function increases the tolerance towards this toxic metalloid.

3.4. *MpACR3 affects the level of As-mediated oxidative stress in M. polymorpha*

To further investigate the status of oxidative stress generated by arsenic exposure, lipid peroxidation assay was carried out by measuring malondialdehyde (MDA) content. First of all, MDA concentration was quantified after three- and five-day exposure with 0 μM or 75 μM AsIII from 10-day-old Cam2 wild-type plants and two independent Mp*acr3* knockout mutant lines. No differences in MDA content were detected under untreated conditions at both time points (Figs. 5A and 5B), but significantly higher concentrations of MDA were observed for Mp*acr3* mutants relative to that of Cam2 after AsIII exposure for both three and five days. The absolute MDA amounts were higher on day five than on day three ($p = 0.00017$ and 1.19×10^{-5} for Mp*acr3–1-5*^{ge} on day 3 and 5, $p = 6.89 \times 10^{-6}$ and $5.79 \times 10–5$ for Mp*acr3–2-1*^{ge} on day 3 and 5 based on Student's *t*-test against Cam2; Figs. 5A and 5B). Mp*ACR3* overexpression lines showed no significant changes in MDA contents compared with Cam2 under control conditions. However, the Cam2 wild-type plants had a significantly higher MDA concentration than Mp*ACR3* overexpression lines upon 1600 μM AsIII exposure ($p = 3.1 \times 10^{-5}$ for Mp*ACR3-ox-9* and $p = 2.55 \times 10^{-5}$ for Mp*ACR3–0x-10*; Fig. 5C). In addition, two more days of exposure with 1600 μM AsIII caused Cam2 plants to completely bleach out, preventing the collection of the data. Taken together, these results indicate that Mp*acr3* knockout lines are more sensitive than Cam2 to arsenic-derived oxidative stress, while Mp*ACR3* overexpression lines are more tolerant than Cam2 to oxidative stress. Thus, MpACR3 plays a positive role in As-derived oxidative stress tolerance.

3.5. *MpACR3 controls the intracellular concentration of arsenic and affects its speciation*

To measure the effect of loss- and gain-of-function of MpACR3 on the intracellular As accumulation we performed two series of experiments. In the first experiment the gametophytes of the different genotypes were exposed to AsIII in the growth medium for three days and then the total As concentration in the plants was measured. Both Mp*acr3* knockout lines accumulated significantly more total As per unit of dry weight than Cam2 plants (Fig. S3A), while no significant difference could be detected between Mp*ACR3* overexpressing plants and the WT (Fig. S3B). In the second experiment, we challenged all genotypes with 10 μM AsV for 24 hr, afterwards we measured the different As species (AsIII and AsV) per unit of dry plant tissue. In this case the total concentrations of As (AsIII + AsV) in the plant inversely correlated with the levels of MpACR3 function: the gain-of-function lines accumulated significantly lower concentrations of As than WT and about two orders of magnitude lower concentrations of As than the loss-of-function lines (Fig. 6A). Interestingly, also the ratios of the different As species correlated with MpACR3 function levels: The gain-of-function lines had a significantly higher AsV/AsIII ratio than both Cam2 and Mp*acr3* mutants, while in the loss-of-function Mp*acr3* mutants virtually all As was present in its reduced form as arsenite (AsIII; Figs. 6B and 6C). Therefore, MpACR3 takes part in regulating the concentration and relative abundance of As species.

3.6. *Tissue-specificity and subcellular localization of MpACR3*

To provide the final proof that MpACR3 is responsible for As detoxification and to try to gain further insights into the mechanisms underlying As tolerance, we complemented one of the loss-of-function Mp*acr3* mutants with the Mp*ACR3* genomic locus encompassing both promoter and gene body (exons and introns) excluding its translation termination codon. The gene locus thus obtained was fused in frame with a C-terminal 3xCitrine fluorescent protein to visualize its expression and subcellular localization by transformation into the Mp*acr3* mutant. Of the eight putative complementation lines, two turned out to be false positives lacking the T-DNA harboring the transgene (Fig. S4) and were used as negative controls alongside with the Cam2 positive control for ACR3 activity to check the levels of tolerance to As. Among the six complementation lines tested, different levels of tolerance were observed, but always not significantly different from Cam2, by contrast to the two negative controls, which were less tolerant to As than Cam2 (Fig. 7), indicating that the MpACR3::3xCitrine is functional.

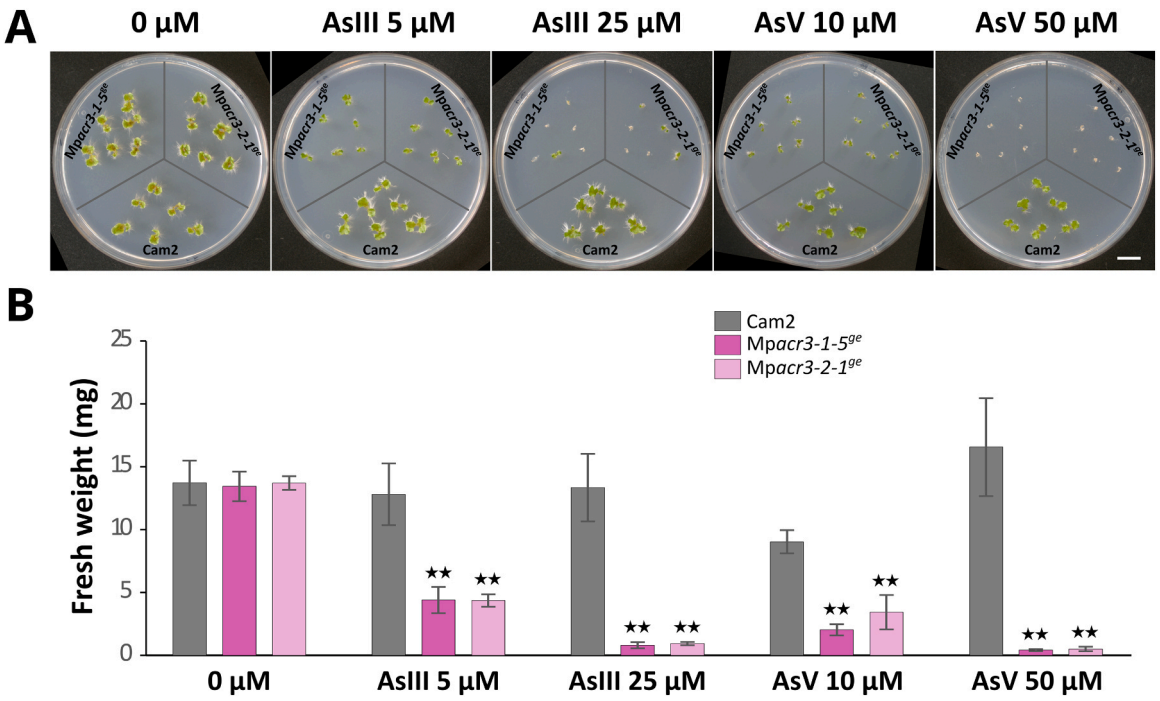

Fig. 3. Phenotype and fresh weight of Mp*acr3* knockout mutants compared with Cam2 wild-type plants under control and As treatments. (A) Representative phenotypes of plants treated with different concentrations of AsIII and AsV; (B) quantification of fresh weight for each genotype. The scale bars indicate 10 mm. Vertical bars in the graphs represent standard deviation (n ≥ 5 biological replicates). Two stars stand for statistically significant difference of the mutant lines from the corresponding Cam2 (Student's *t*-test, P < 0.01).

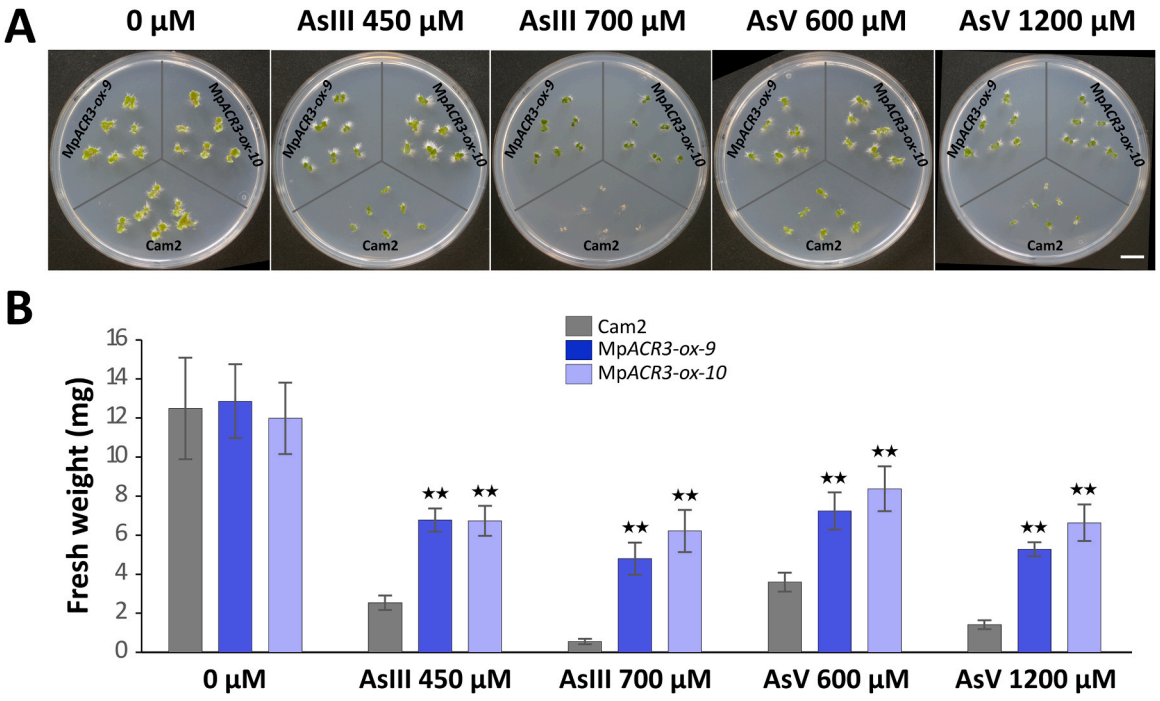

Fig. 4. Phenotypes and fresh weight of two selected transgenic lines overexpressing Mp*ACR3* in *M. polymorpha* compared with Cam2 wild-type plants under control and As treatments. (A) Representative phenotypes under different concentrations of AsIII and AsV treatments. The scale bar indicates 10 mm. (B) Quantification of fresh weight for the corresponding genotypes. Colored and error bars in the graphs represent average and standard deviation, respectively (n ≥ 5 biological replicates). Two stars indicate a significant difference of the transgenic lines from the corresponding Cam2 (Student's *t*-test, P < 0.01).

Complementation line C1 was used for visualizing the tissue-specific expression domains given its high fluorescent signal, while line C5, with weaker fluorescence levels, was selected for subcellular localization analyses to avoid possible artifacts due to excessively strong expression. In the C1 line gemmae, Citrine fluorescence signal were visible mainly around the apical notch (meristematic region) of the gemma, while they were very low in the rest of the cells (Supplementary Fig. S5A), including the ventral rhizoids. Barely detectable expression

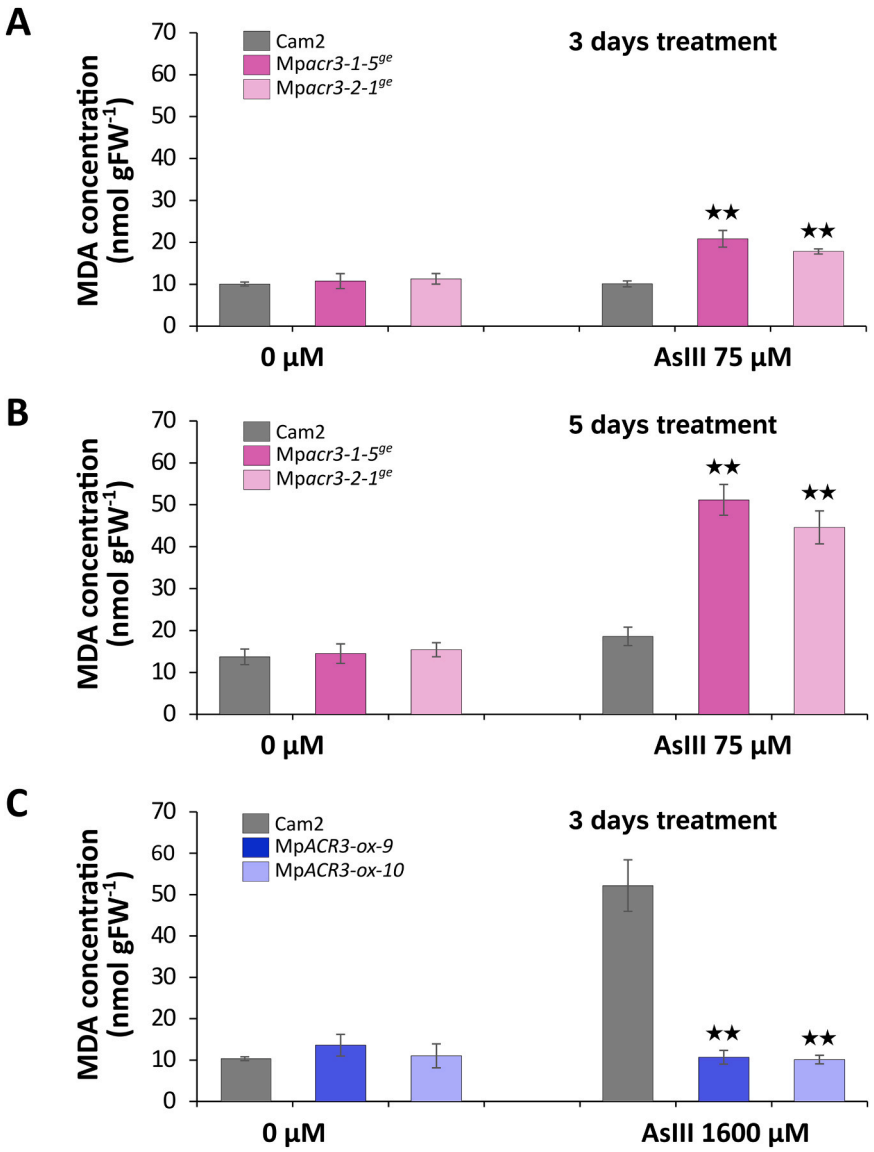

Fig. 5. Lipid peroxidation assay from ten-day-old Cam2 wild-type plants, Mp*acr3* knockout mutants and Mp*ACR3* overexpression lines in *M. polymorpha* treated without or with AsIII. MDA concentration measured from Cam2 and two Mp*acr3* mutant lines exposed without or with 75 µM AsIII for three days in (A) and five days in (B). (C) represents the MDA concentration derived from Cam2 and two MpACR3 overexpression lines treated without or with 1600 µM AsIII for three days. Bars specify standard deviation (n = 4 biological replicates), two stars indicate very significant difference from Cam2 wild-type plants (Student's *t*-test, $P < 0.01$).

was observed in the rhizoids (Supplementary Fig. S5B). At the subcellular level, the MpACR3::3xCitrine-derived signal was localized at the periphery of the cells (Figs. 8A and 8B), but below the cell wall stained with PI (Fig. 8C), in agreement with a plasma membrane localization. Part of the Citrine fluorescence was also localized in the inner part of the cell, in some endomembrane systems (Fig. 8B), possibly because of slow and/or partial folding of the bulky 3xCitrine tag.

3.7. The Mpacr3 mutants could be used as visual bioindicators of drinking water As contamination

Given the high and differential sensitivity shown by the *M. polymorpha* Mp*acr3* mutants compared to WT Cam2, we tested whether they could be used as bioindicators of As contamination in drinking water. For these experiments, we used oligo-mineral water and 10 µM of either AsV (the most common arsenic form in oxidant conditions) or AsIII (the dominant form in anoxigenic conditions). In both cases, after 8 days of growth in control conditions, no differences in growth could be observed among WT Cam2 and the mutant lines Mp*acr3–1-5*^{ge} and Mp*acr3–2-1*^{ge} (Fig. 9). In contrast, both the AsIII and AsV treatment resulted in large differences in size easily observed by naked eye between WT Cam2 (large) and the mutants (small; Fig. 9). Our results indicate that these two genotypes could be conveniently used to detect potential As contamination in drinking groundwater comparable to those found in countries like India and Bangladesh [4,32].

4. Discussion

In the perennial struggle for darwinian survival, the fundamental role of gene and genome duplication as fuel for the emergence of novel traits with adaptive value has been often emphasized, but recent evidence gained from comparative genomics of the two major lineages of land plants, bryophytes and tracheophytes, is prompting re-evaluating the importance of gene loss in reductive and possibly adaptive evolution of plants [16]. While the major gene losses happened in bryophytes, resulting in simplified body plans, multiple trait losses and generally low level of genetic redundancy (although with the notable exception of mosses; [42]), a number of traits were lost also during the evolution of

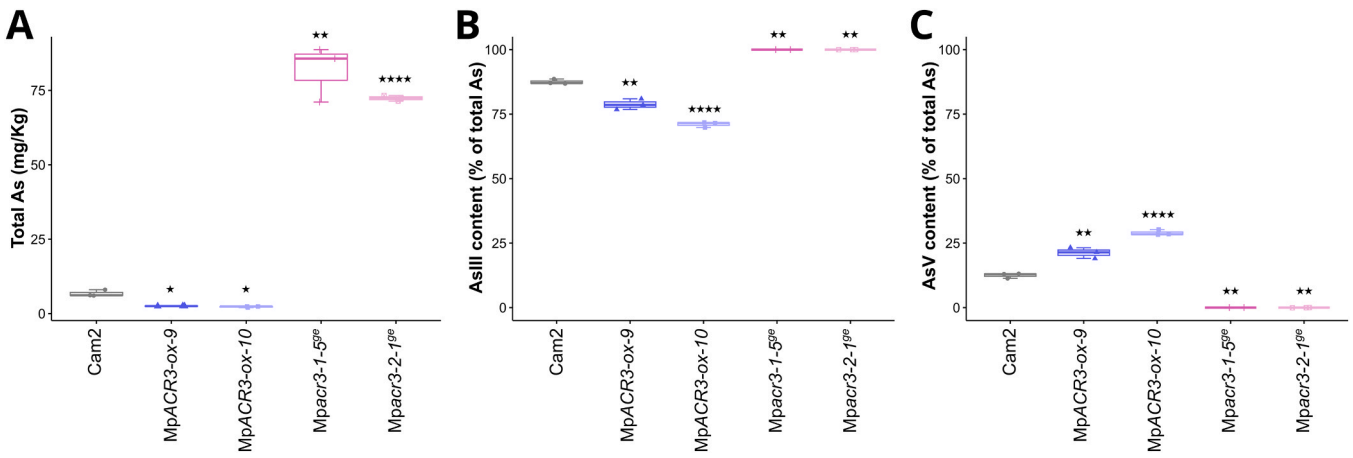

Fig. 6. Arsenic species content of transgenic *M. polymorpha* lines with gain- and loss-of-function of *MpACR3*. The WT *M. polymorpha* ecotype (Cam2), two independent transgenic lines overexpressing *MpACR3* (Mp*ACR3-ox-9* and Mp*ACR3-ox-10*) and two independent *Mpacr3* knockout mutants (Mp*acr3–1-5*^{ge} and Mp*acr3–2-1*^{ge}) were treated with 10 μM AsV for 24 h and then the amounts of AsIII and AsV species present in the plants were measured. (A) Total As content (AsIII + AsV) expressed in mg of As per Kg of dry plant tissue. (B) Percentage of AsIII with respect to the total As contained in the different genotypes. (C) Percentage of AsV with respect to the total As contained in the different genotypes. The boxplots are calculated from three biological replicates. The number of stars corresponds to the level of statistical significance of a Student's *t*-test between the As content for each genotype compared to that of WT Cam2 plants. * : $p <= 0.05$; **: $p <= 0.01$; *** : $p <= 0.001$; ****: $p <= 0.0001$.

angiosperms (e.g. [26,57,46,69,62]).

However, while the majority of these reported losses are lineage-specific, only few correspond to cases where trait loss coincided with the origin of angiosperms and the trait is missing in all angiosperm species (e.g. [44]). In such rare cases, trait loss might have played a role in angiosperm evolution or might have simply happened by accident contextually to their radiation.

Whether the *ACR3* gene was lost incidentally or under a yet unknown type of selective pressure at the beginning of angiosperm radiation remains an open question. A first step towards a possible answer is to determine if the gene function deduced from *P. vittata* (a representative of the tracheophytes) is shared by bryophytes, too. Since *P. vittata* is the most extreme As hyperaccumulator known to date, it might, in fact, not constitute the ideal model to fully elucidate *ACR3* function or mechanism of action in the majority of land plants where it exists. The high level of homology and phylogenetic relationships observed in this study for Mp*ACR3* with respect to representative bryophytes and tracheophyte species (Figs. 1A and 1B), clearly exclude that the *M. polymorpha* gene could be a result of horizontal gene transfer, as it is instead the case for the multiple *ACR3* copies found in arsenic hypertolerant and acidophilic unicellular alga *Chlamydomonas eustigma* Ettl [30]. Several lines of evidence indicate that Mp*ACR3* shares various functional features with its homologues from *P. vittata*. Like the plasma-membrane localized copies *PvACR3* and *PvACR3;2* from *P. vittata*, also Mp*ACR3* transcription is upregulated by arsenic [17,33].

It is important to note that the differences in upregulation by AsIII and AsV we observed (Figs. 2B and 2C) cannot be compared in absolute terms, as they provide only a qualitative indication of the ability of both As reduction states to activate Mp*ACR3* transcription in the particular experimental conditions used: the two As forms, in fact, are taken up by the plant cells with completely different transport systems, undergo different routes for detoxification and display different toxicity levels [65]. Another feature in common between Mp*ACR3* and *PvACR3* is their fundamental role in As detoxification. While the molecular tools available for *P. vittata* did not allow for stable transformation and therefore no stable overexpressing lines could be obtained, downregulation by RNAi of *PvACR3* caused hypersensitivity to As in *P. vittata* [33] like CRISPR-CAS9 mediated Mp*acr3* knockouts made *M. polymorpha* extremely susceptible to As treatment (Figs. 3A and 3B).

While the phenotype observed in *P. vittata* may have in principle stemmed from the silencing of multiple *ACR3* paralogues given the relatively low specificity of the RNAi technique [19], in our study the use of two different targets for the Mp*ACR3* knockout guarantees an absolute specificity (Fig. S1). In addition, the Mp*ACR3* gain of function generated by overexpression consistently confers the opposite phenotype, i.e. increased tolerance to As (Figs. 4A and 4B), and complementation of one of the mutants with the genomic locus tagged with a C-Terminal 3xCitrine fluorescent marker complement its As hypersensitivity (Fig. 7 and Supplementary Fig. S4). Taken together, these results demonstrate that Mp*ACR3* is a major positive player in the detoxification of arsenic in *M. polymorpha*. As the single *ACR3* gene present in *S. cerevisiae* and the non-hyperaccumulator *Pteris ensiformis* Burm.f. are located at the plasma membrane where they actively extrude AsIII from the cytoplasm [47,65], the mechanism of action of the single Mp*ACR3* of *M. polymorpha* could be similar. In support of this hypothesis, loss-of-function Mp*acr3* mutants accumulate much more total As per unit of dry weight than Cam2 WT (Figs. S3A and 6A), despite the consequent toxicity dramatically decreasing their growth (Figs. 3A and 3B). Interestingly, also under control conditions, the mutants accumulate significantly higher amounts of As than the WT despite no significant growth differences, possibly due to trace contamination from water or glassware (Fig. S3A).

We attribute the lack of difference in total As in the Mp*ACR3* overexpressing lines in Fig. S3A to the high concentration of As used in the treatment, which saturates both the WT and the overexpressing lines capacity to extrude AsIII from the cytoplasm, despite the pretty high levels of Mp*ACR3* expression under normal conditions (Fig. 2A and Supplementary Fig. S2). In support of the saturation effect, at lower As concentrations in the medium, the overexpression lines did show a lower content of As per unit of dry weight (Fig. 6A). Noteworthy, the function of MpACR3 is also inversely related to the relative proportion of the As species (AsIII and AsV) present in the cell. As the treatment was carried out with AsV, it seems that the AsV present in the cytoplasm can stimulate transcription and/or activity of the HAC1 reductase, because in the Mp*acr3* mutant genotypes (containing much more total arsenic in the cytoplasm than the other genotypes; Fig. 6A) all As is in the form of arsenite, while in the overexpressing lines (with slightly less total arsenic than the WT; Fig. 6A) a lower proportion of AsV is reduced to AsIII (Figs. 6B and 6C).

In support of this conclusion, in *Arabidopsis* and *P. vittata* the expression of *HAC1* is strongly upregulated by arsenate [11,40], and also *HAC1;1* expression is moderately induced by AsV in rice [63]. In

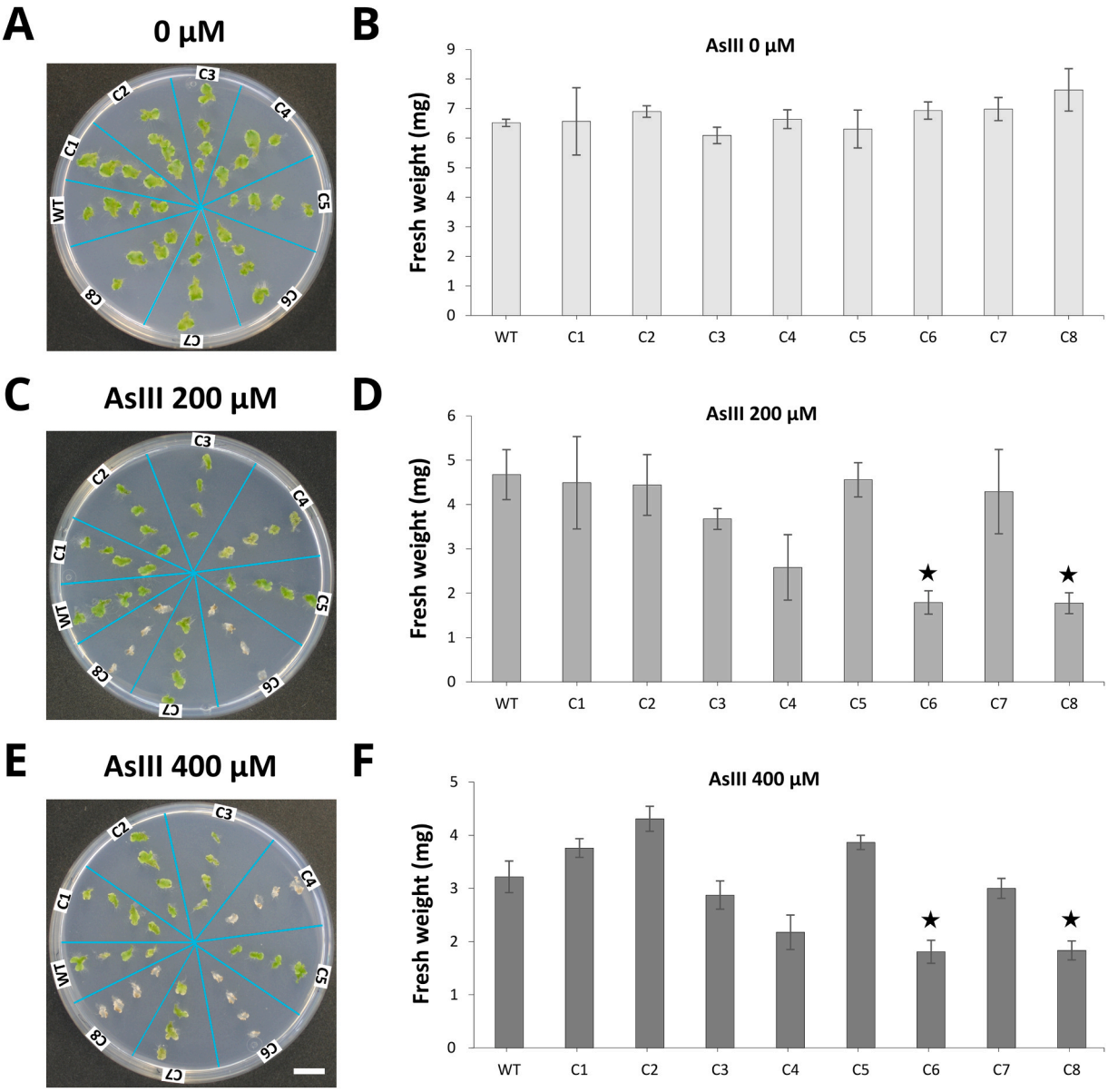

Fig. 7. Phenotype and fresh weigh of eight independent lines complemented with the Mp*ACR3* genomic locus tagged with a 3xCitrine C-terminal fusion in the Mp*acr3–1-5*^{ge} genetic background. Indicative images of the phenotype upon treatment with different concentrations of AsIII are provided in panels A, C, and E. Fresh weight measurements were carried out after one week exposure to the indicated AsIII concentration for 16-day-old Cam2 and complementation lines in B, D, and F. Bars specify standard deviation (n = 4 biological replicates), while stars represent significant differences from Cam2 wild-type plants (Student's *t*-test, $P < 0.05$).

summary, the above observations suggest that activity of MpACR3 plays a pivotal role in As detoxification, regulating not only the total amount of As in the plants, but also affecting the speciation of As in the cell. Analysis of the subcellular localization in the complementation lines suggests that the MpACR3::3xCitrine-derived signal observed at the cell periphery below the cell wall is consistent with a plasma membrane localization (Fig. 8). This is in line with the decrease of total As in the overexpressing lines and the strong increase of AsIII accumulation in the knockout mutants (Fig. 6A, B and C), both results fully compatible with the capacity of MpACR3 to extrude AsIII from the cytoplasm. The intracellular fluorescent signals observed in cells of the strong MpACR3::3xCitrine expressor complemented line are compatible with either cytoplasmic or endoplasmic reticulum localization of the protein fusion (Supplementary Fig. S5), maybe because of the bulk and high hydrophobicity of the 3xCitrine tags fused to MpACR3 C-Terminal could interfere with proper folding/localization of a pool of the expressed protein.

Besides the hyperaccumulator *P. vittata*, the only two other non-hyperaccumulator species characterized to date and natively possessing a single copy of ACR3 are *S. cerevisiae* and *P. ensiformis* [47,65,70]. While in yeast the plasma membrane localization of the ACR3 protein has been ascertained [47], for *P. ensiformis* PeACR3 localization has been till now only proposed but not confirmed [65]. If, as in *M. polymorpha*, ACR3 in *P. ensiformis* is localized to the plasma membrane [65], this would raise the question of whether additional mechanisms guarantee the capacity of WT *M. polymorpha* to withstand high As concentrations. As MpACR3 proteins, like all other plant ACR3, have a deletion in correspondence of ScACR3 cytoplasmic loop #4 which mediates the feedback regulation of As intake by the FPS1 aquaporin [37], a reduced intake by downregulation of plasma membrane aquaporins at the moment seems unlikely in *M. polymorpha*.

Irrespective of the specific mechanism of action in the WT, the Mp*acr3* loss-of-function obtained in this work are hypersensitive to concentrations of As that make them a complementary addition to the

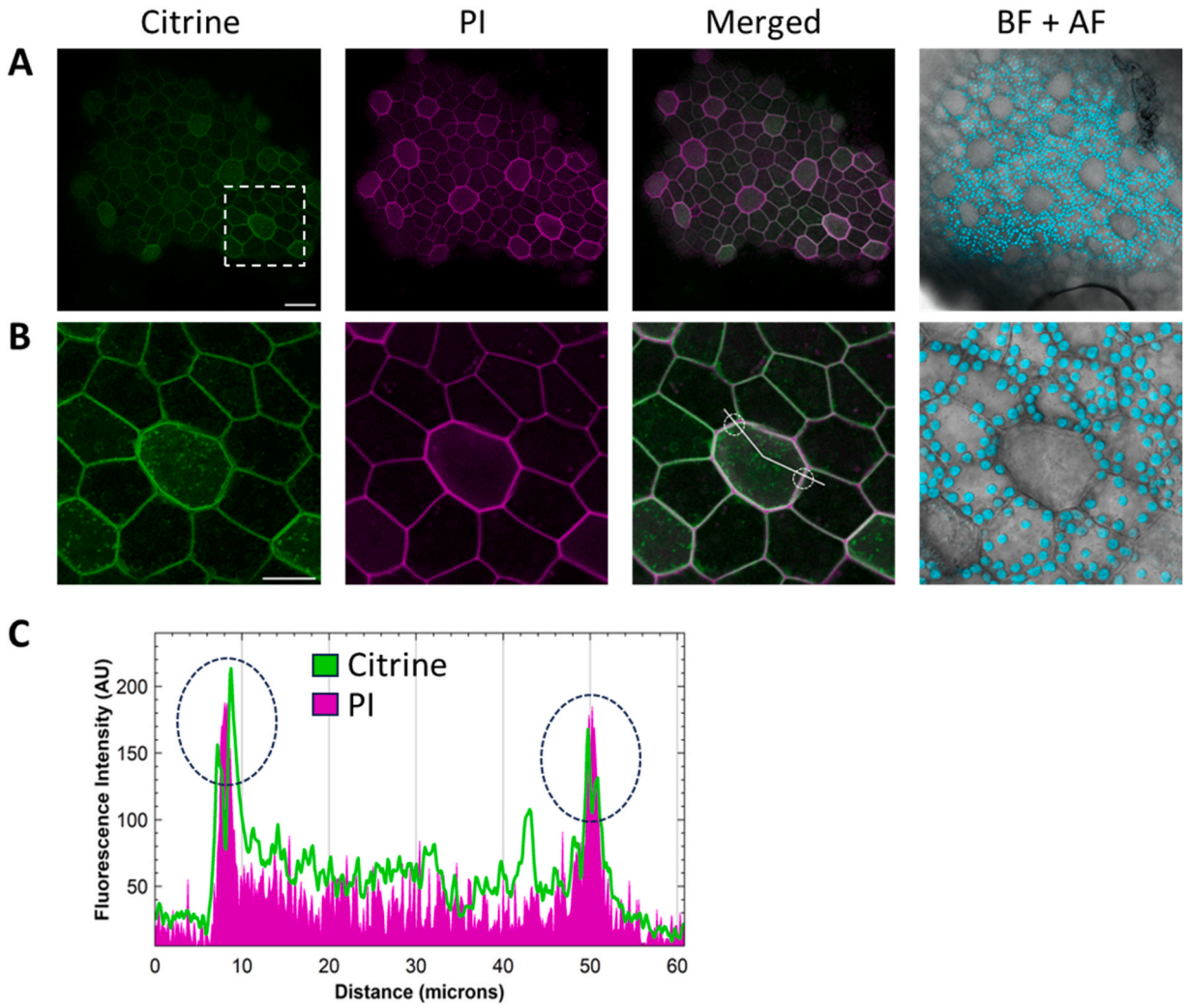

Fig. 8. Subcellular localization of MpACR3. The complementation line C5 was used to assess the subcellular localization of the MpACR3::3xCitrine protein fusion in the gemmae of the Mp*acr3* mutant. A: From left to right panels, MpACR3::3xCitrine, green channel; propidium iodide at 0005%, magenta channel; Merged of Citrine and PI; Merged of bright field (BF, gray) and chlorophyll autofluorescence (AF, cyan) images. Scale bar = 50 μm. B: Close up of white box drawn in A. Same panel sequence. Scale bar = 25 μm. C: Fluorescence intensity plot in arbitrary units (AU) over the line drawn in B for both the Citrine (green) and PI (magenta) channels. Note how the magenta PI peaks at the cell borders (dashed black and white circles in C and B, respectively) are sandwiched between the citrine peaks of adjacent cells consistent with the two plasma membranes of the adjacent cells surrounding the common primary cell wall.

previously obtained Mp*pcs* mutants, which are hypersensitive to cadmium [39]. As in the case of the Mp*pcs* mutants, segregation of the T-DNA by crossing to WT Cam1 (male) plants, will allow us to obtain transgene-free Mp*acr3* mutants, which according to the laws in many countries (e.g. USA and Europe; for Europe, please see https://www.europarl.europa.eu/doceo/document/TA-9–2024-0067_EN.pdf) are classified as NGT1 (new genomic techniques type 1) non-genetically modified plants. Additionally, we envision that especially for water contamination, the water to be tested can be brought to the laboratory/facility for analysis, so there is not even the need to bring the NGT1 mutants into the external environment. In this study, we tested exposure of the mutants (Mp*pcr3–2-1*^{ge} and Mp*acr3–1-5*^{ge}; see Fig. 9) to oligomineral water containing AsIII at a concentration of 10 μM, which corresponds to levels of As contamination found in 5–6% of groundwater in countries like India and Bangladesh [4,32]. At this concentration (and even 5 μM in solid medium; see Figs. 3A and 3B) the growth of the mutants is significantly retarded compared to that of WT, indicating that the Mp*acr3* mutants can be used as low-cost biosensors to detect medium to high As concentrations in water. With the growing knowledge of the mechanisms involved in As detoxification in *M. polymorpha*, it could be possible to further enhance the specificity of novel mutant-based As-bioindicators. We envision that the growing set of heavy-metal (loid) bioindicator lines of *M. polymorpha* (until now specific for cadmium and arsenic) will lead to a broader and cheaper ability to screen or pre-screen without direct chemical analyses for heavy metal(loid) environmental pollution in low-income countries, thus helping to decrease human exposure to these highly toxic elements.

Environmental implication

Inorganic arsenic (As) is a recognized carcinogen, considered the most hazardous element at the global level due to its ubiquitous presence as environmental pollutant of either natural or anthropic origin. The current work extends previous studies carried out in our lab for the creation of a series of biosensors based on mutants of the ACR3 arsenite transporter in the bryophyte *Marchantia polymorpha*. Mp*acr3* mutants are extremely susceptible to As at levels that in some countries can be found in drinking water, resulting in a cheap and low-technology biosensor potentially useful to people worldwide for detecting As-contaminated water.

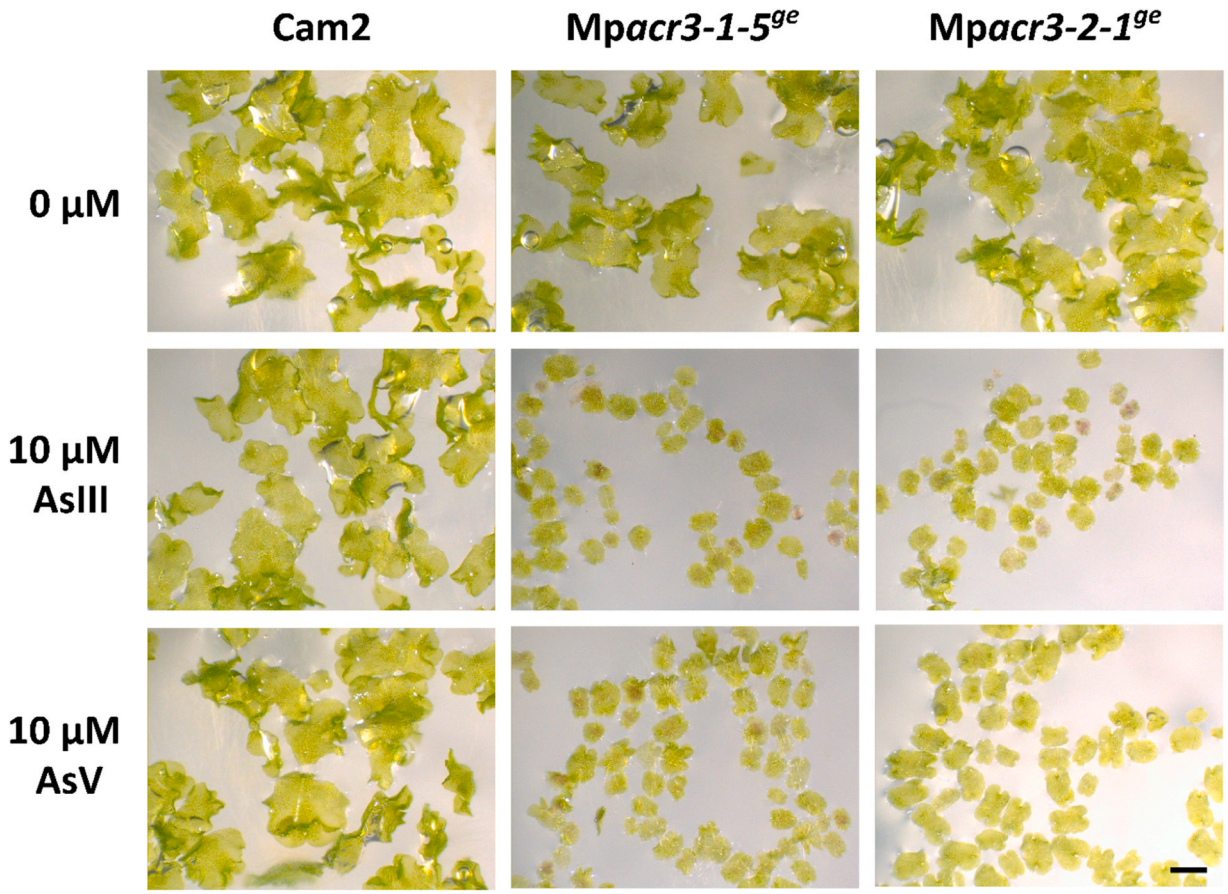

Fig. 9. Phenotypes of Cam2 WT plants and two Mpacr3 knockout mutants after growth in oligomineral water for 8 days with or without the addition of 10 µM of AsIII or AsV. Scale bar = 3 mm.

CRediT authorship contribution statement

Daniela Bertoldi: Writing – review & editing, Writing – original draft, Investigation, Formal analysis. **Aurélien Boisson-Dernier:** Writing – review & editing, Writing – original draft, Investigation, Visualization, Funding acquisition. **Mingai Li:** Writing – review & editing, Writing – original draft, Visualization, Validation, Supervision, Project administration, Investigation, Formal analysis, Conceptualization. **Claudio Varotto:** Writing – review & editing, Writing – original draft, Visualization, Validation, Supervision, Resources, Project administration, Funding acquisition, Formal analysis, Conceptualization. **Marco Grotti:** Writing – review & editing, Writing – original draft, Supervision, Resources. **Roberto Larcher:** Writing – review & editing, Writing – original draft, Supervision, Resources. **Francisco Ardini:** Writing – review & editing, Writing – original draft, Investigation, Formal analysis.

Declaration of Competing Interest

The authors declare that they have no known competing financial interests or personal relationships that could have appeared to influence the work reported in this paper.

Data Availability

All the relevant data are already in the article and its supplementary files.

Acknowledgements

The authors would like to thank Enrico Barbaro for technical support. This work was supported by the Autonomous Province of Trento (core funding to the Ecogenomics Unit). Work in ABD lab was supported by the French government through the France 2030 investment plan managed by the National Research Agency (ANR), as part of the Initiative of Excellence Université Côte d'Azur under reference number ANR-15-IDEX-01.

Appendix A. Supporting Information

Supplementary data associated with this article can be found in the online version at doi:10.1016/j.jhazmat.2024.134088.

References

[1] Aboul-Maaty, N.A.-F., Oraby, H.A.-S., 2019. Extraction of high-quality genomic DNA from different plant orders applying a modified CTAB-based method. Bull Natl Res Cent 43, 25.
[2] Altschul, S.F., Gish, W., Miller, W., Myers, E.W., Lipman, D.J., 1990. Basic local alignment search tool. J Mol Biol 215, 403–410.
[3] Bali, A.S., Sidhu, G.P.S., 2021. Arsenic acquisition, toxicity and tolerance in plants - From physiology to remediation: a review. Chemosphere 283, 131050.
[4] Basu, A., Saha, D., Saha, R., Ghosh, T., Saha, B., 2014. A review on sources, toxicity and remediation technologies for removing arsenic from drinking water. Res Chem Intermed 40, 447–485.
[5] Bellini, E., Bandoni, E., Giardini, S., Sorce, C., Spanò, C., Bottega, S., Fontanini, D., Kola, A., Valensin, D., Bertolini, A., et al., 2023. Glutathione and phytochelatins jointly allow intracellular and extracellular detoxification of cadmium in the liverwort Marchantia polymorpha. Environ Exp Bot 209, 105303.
[6] Bellini, E., Varotto, C., Borsò, M., Rugnini, L., Bruno, L., Sanità di Toppi, L., 2020. Eukaryotic and prokaryotic phytochelatin synthases differ less in functional terms

than previously thought: a comparative analysis of marchantia polymorpha and Geitlerinema sp. PCC 7407. Plants 9, 914.
[7] Benson, D.A., Karsch-Mizrachi, I., Lipman, D.J., Ostell, J., Rapp, B.A., Wheeler, D. L., 2000. GenBank. Nucleic Acids Res 28, 15–18.
[8] Bobrowicz, P., Wysocki, R., Owsianik, G., Goffeau, A., Ułaszewski, S., 1997. Isolation of three contiguous genes, ACR1, ACR2 and ACR3, Involved in resistance to arsenic compounds in the yeast saccharomyces cerevisiae. Yeast 13, 819–828.
[9] Bowman, J.L., Arteaga-Vazquez, M., Berger, F., Briginshaw, L.N., Carella, P., Aguilar-Cruz, A., Davies, K.M., Dierschke, T., Dolan, L., Dorantes-Acosta, A.E., et al., 2022. The renaissance and enlightenment of Marchantia as a model system. Plant Cell 34, 3512–3542.
[10] Bowman, J.L., Kohchi, T., Yamato, K.T., Jenkins, J., Shu, S., Ishizaki, K., Yamaoka, S., Nishihama, R., Nakamura, Y., Berger, F., et al., 2017. Insights into Land plant evolution garnered from the marchantia polymorpha genome. Cell 171, 287–304.e15.
[11] Chao, D.-Y., Chen, Y., Chen, J., Shi, S., Chen, Z., Wang, C., Danku, J.M., Zhao, F.-J., Salt, D.E., 2014. Genome-wide association mapping identifies a new arsenate reductase enzyme critical for limiting arsenic accumulation in plants. PLoS Biol 12, e1002009.
[12] Chao, Y.-S., Liu, H.-Y., Chiang, Y.-C., Chiou, W.-L., 2012. Polyploidy and Speciation in *Pteris* (Pteridaceae). J Bot 2012, e817920.
[13] Chen, J.-X., Cao, Y., Yan, X., Chen, Y., Ma, L.Q., 2021. Novel PvACR3;2 and PvACR3;3 genes from arsenic-hyperaccumulator Pteris vittata and their roles in manipulating plant arsenic accumulation. J Hazard Mater 415, 125647.
[14] Chen, Y., Hua, C.-Y., Jia, M.-R., Fu, J.-W., Liu, X., Han, Y.-H., Liu, Y., Rathinasabapathi, B., Cao, Y., Ma, L.Q., 2017. Heterologous expression of pteris vittata arsenite antiporter PvACR3;1 reduces arsenic accumulation in plant shoots. Environ Sci Technol 51, 10387–10395.
[15] Chen, Y., Xu, W., Shen, H., Yan, H., Xu, W., He, Z., Ma, M., 2013. Engineering arsenic tolerance and hyperaccumulation in plants for phytoremediation by a PvACR3 transgenic approach. Environ Sci Technol 47, 9355–9362.
[16] Clark, J.W., 2023. Genome evolution in plants and the origins of innovation. N Phytol 240, 2204–2209.
[17] Dai, Z.-H., Peng, Y.-J., Ding, S., Chen, J.-Y., He, S.-X., Hu, C.-Y., Cao, Y., Guan, D.-X., Ma, L.Q., 2022. Selenium increased arsenic accumulation by upregulating the expression of genes responsible for arsenic reduction, translocation, and sequestration in arsenic hyperaccumulator pteris vittata. Environ Sci Technol 56, 14146–14153.
[18] Del Rio, M., Alvarez, J., Mayorga, T., Dominguez, S., Sobin, C., 2017. A comparison of arsenic exposure in young children and home water arsenic in two rural West Texas communities. BMC Public Health 17, 850.
[19] Dillin, A., 2003. The specifics of small interfering RNA specificity. Proc Natl Acad Sci 100, 6289–6291.
[20] Donoghue, P.C.J., Harrison, C.J., Paps, J., Schneider, H., 2021. The evolutionary emergence of land plants. Curr Biol 31, R1281–R1298.
[21] EFSA Panel on Contaminants in the Food Chain (CONTAM), 2009. Scientific opinion on arsenic in food. EFSA J 7, 1351.
[22] Fasani, E., Li, M., Varotto, C., Furini, A., DalCorso, G., 2022. Metal detoxification in land plants: from bryophytes to vascular plants. state of the art and opportunities. Plants 11, 237.
[23] Garbinski, L.D., Rosen, B.P., Chen, J., 2019. Pathways of arsenic uptake and efflux. Environ Int 126, 585–597.
[24] Goffinet, B., 2008. Bryophyte Biology. Cambridge University Press.
[25] Goodstein, D.M., Shu, S., Howson, R., Neupane, R., Hayes, R.D., Fazo, J., Mitros, T., Dirks, W., Hellsten, U., Putnam, N., et al., 2012. Phytozome: a comparative platform for green plant genomics. Nucleic Acids Res 40, 1178–1186.
[26] Griesmann, M., Chang, Y., Liu, X., Song, Y., Haberer, G., Crook, M.B., Billault-Penneteau, B., Lauressergues, D., Keller, J., Imanishi, L., et al., 2018. Phylogenomics reveals multiple losses of nitrogen-fixing root nodule symbiosis. Science 361, eaat1743.
[27] Guindon, S., Dufayard, J.F., Lefort, V., Anisimova, M., Hordijk, W., Gascuel, O., 2010. New algorithms and methods to estimate maximum-likelihood phylogenies: assessing the performance of PhyML 3.0. Syst Biol 59, 307–321.
[28] Harris, B.J., Clark, J.W., Schrempf, D., Szöllősi, G.J., Donoghue PCJ, Hetherington, A.M., Williams, T.A., 2022. Divergent evolutionary trajectories of bryophytes and tracheophytes from a complex common ancestor of land plants. Nat Ecol Evol 1–10.
[29] Hayashi, S., Kuramata, M., Abe, T., Takagi, H., Ozawa, K., Ishikawa, S., 2017. Phytochelatin synthase OsPCS1 plays a crucial role in reducing arsenic levels in rice grains. Plant J 91, 840–848.
[30] Hirooka, S., Hirose, Y., Kanesaki, Y., Higuchi, S., Fujiwara, T., Onuma, R., Era, A., Ohbayashi, R., Uzuka, A., Nozaki, H., et al., 2017. Acidophilic green algal genome provides insights into adaptation to an acidic environment. Proc Natl Acad Sci 114, E8304–E8313.
[31] Hodges, D.M., DeLong, J.M., Forney, C.F., Prange, R.K., 1999. Improving the thiobarbituric acid-reactive-substances assay for estimating lipid peroxidation in plant tissues containing anthocyanin and other interfering compounds. Planta 207, 604–611.
[32] Hossain, M.F., 2006. Arsenic contamination in Bangladesh—an overview. Agric, Ecosyst Environ 113, 1–16.
[33] Indriolo, E., Na, G.N., Ellis, D., Salt, D.E., Banks, J.A., 2010. A vacuolar arsenite transporter necessary for arsenic tolerance in the arsenic hyperaccumulating fern Pteris vittata is missing in flowering plants. Plant Cell 22, 2045–2057.
[34] Ishizaki, K., Nishihama, R., Ueda, M., Inoue, K., Ishida, S., Nishimura, Y., Shikanai, T., Kohchi, T., 2015. Development of gateway binary vector series with four different selection markers for the liverwort Marchantia polymorpha. PLoS ONE 10, 1–13.
[35] Katoh, K., Rozewicki, J., Yamada, K.D., 2018. MAFFT online service: multiple sequence alignment, interactive sequence choice and visualization. Brief Bioinforma 20, 1160–1166.
[36] Kubota, A., Ishizaki, K., Hosaka, M., Kohchi, T., 2013. Efficient agrobacterium-mediated transformation of the liverwort marchantia polymorpha using regenerating thalli. Biosci, Biotechnol, Biochem 77, 167–172.
[37] Lee, J., Levin, D.E., 2022. Differential metabolism of arsenicals regulates Fps1-mediated arsenite transport. J Cell Biol 221, e202109034.
[38] Li, M., Barbaro, E., Bellini, E., Saba, A., Sanità di Toppi, L., Varotto, C., 2020. Ancestral function of the phytochelatin synthase C-terminal domain in inhibition of heavy metal-mediated enzyme overactivation (A Cuypers, Ed. J Exp Bot 71, 6655–6669.
[39] Li, M., Leso, M., Buti, M., Bellini, E., Bertoldi, D., Saba, A., Larcher, R., Sanità di Toppi, L., Varotto, C., 2022. Phytochelatin synthase de-regulation in Marchantia polymorpha indicates cadmium detoxification as its primary ancestral function in land plants and provides a novel visual bioindicator for detection of this metal. J Hazard Mater 440, 129844.
[40] Li, X., Sun, D., Feng, H., Chen, J., Chen, Y., Li, H., Cao, Y., Ma, L.Q., 2020. Efficient arsenate reduction in As-hyperaccumulator Pteris vittata are mediated by novel arsenate reductases PvHAC1 and PvHAC2. J Hazard Mater 399, 122895.
[41] Linde, A.-M., Eklund, D.M., Cronberg, N., Bowman, J.L., Lagercrantz, U., 2021. Rates and patterns of molecular evolution in bryophyte genomes, with focus on complex thalloid liverworts, Marchantiopsida. Mol Phylogenetics Evol 165, 107295.
[42] Linde A.-M. , Singh S. , Bowman J.L. , Eklund M. , Cronberg N. , Lagercrantz U. 2023. Genome Evolution in Plants: Complex Thalloid Liverworts (Marchantiopsida) (Y Van De Peer, Ed.). Genome Biology and Evolution 15: evad014.
[43] Liu, C.-J., Peng, Y.-J., Hu, C.-Y., He, S.-X., Xiao, S.-F., Li, W., Deng, S.-G., Dai, Z.-H., Ma, L.Q., 2023. Copper enhanced arsenic-accumulation in As-hyperaccumulator Pteris vittata by upregulating its gene expression for As uptake, translocation, and sequestration. J Hazard Mater 460, 132484.
[44] Lou, H., Song, L., Li, X., Zi, H., Chen, W., Gao, Y., Zheng, S., Fei, Z., Sun, X., Wu, J., 2023. The Torreya grandis genome illuminates the origin and evolution of gymnosperm-specific sciadonic acid biosynthesis. Nat Commun 14, 1315.
[45] Ma, L.Q., Komar, K.M., Tu, C., Zhang, W., Cai, Y., Kennelley, E.D., 2001. A fern that hyperaccumulates arsenic. Nature 409, 579–579.
[46] Ma X. , Vanneste S. , Chang J. , Ambrosino L. , Barry K. , Bayer T. , Bobrov A.A. , Boston L. , Campbell J.E. , Chen H. , *et al.* 2023. Seagrass genomes reveal a hexaploid ancestry facilitating adaptation to the marine environment.: 2023.03.05.531170.
[47] Maciaszczyk-Dziubinska, E., Migocka, M., Wysocki, R., 2011. Acr3p is a plasma membrane antiporter that catalyzes As(III)/H+ and Sb(III)/H+ exchange in Saccharomyces cerevisiae. Biochim Et Biophys Acta (BBA) - Biomembr 1808, 1855–1859.
[48] Mathur, J., Khare, P.B., Panwar, A., Ranade, S.A., 2021. Analysis of genetic variability amongst polyploid genotypes of pteris vittata l. from various geographic locales of India. Front Ecol Evol 9.
[49] Mizio, K., Wawrzycka, D., Staszewski, J., Wysocki, R., Maciaszczyk-Dziubinska, E., 2023. Identification of amino acid substitutions that toggle substrate selectivity of the yeast arsenite transporter Acr3. J Hazard Mater 456, 131653.
[50] Moon, K.A., Oberoi, S., Barchowsky, A., Chen, Y., Guallar, E., Nachman, K.E., Rahman, M., Sohel, N., D'Ippoliti, D., Wade, T.J., et al., 2017. A dose-response meta-analysis of chronic arsenic exposure and incident cardiovascular disease. Int J Epidemiol 46, 1924–1939.
[51] Nachman, K.E., Ginsberg, G.L., Miller, M.D., Murray, C.J., Nigra, A.E., Pendergrast, C.B., 2017. Mitigating dietary arsenic exposure: current status in the United States and recommendations for an improved path forward. Sci Total Environ 581–582, 221–236.
[52] Nachman, K.E., Punshon, T., Rardin, L., Signes-Pastor, A.J., Murray, C.J., Jackson, B.P., Guerinot, M.L., Burke, T.A., Chen, C.Y., Ahsan, H., et al., 2018. Opportunities and challenges for dietary arsenic intervention. Environ Health Perspect 126, 084503.
[53] Perera, A.J.D., Li, L., Carey, M., Moreno-Jiménez, E., Flagmeier, M., Marwa, E., De Silva, P.M.C.S., Nguyen, M.N., Meharg, A.A., Meharg, C., 2023. Trans-global biogeochemistry of soil to grain transport of arsenic and cadmium. Expo Health.
[54] Podgorski, J., Berg, M., 2020. Global threat of arsenic in groundwater. Science 368, 845–850.
[55] Poli, M., Salvi, S., Li, M., Varotto, C., 2017. Selection of reference genes suitable for normalization of qPCR data under abiotic stresses in bioenergy crop Arundo donax L. Sci Rep 7 (1), 11.
[56] Pourret, O., Bollinger, J.-C., Hursthouse, A., 2021. Heavy metal: a misused term? Acta Geochim 40, 466–471.
[57] Povilus, R.A., DaCosta, J.M., Grassa, C., Satyaki, P.R.V., Moeglein, M., Jaenisch, J., Xi, Z., Mathews, S., Gehring, M., Davis, C.C., et al., 2020. Water lily (Nymphaea thermarum) genome reveals variable genomic signatures of ancient vascular cambium losses. Proc Natl Acad Sci 117, 8649–8656.
[58] Saint-Marcoux, D., Proust, H., Dolan, L., Langdale, J.A., 2015. Identification of Reference Genes for Real-Time Quantitative PCR Experiments in the Liverwort Marchantia polymorpha. PLOS ONE 10, e0118678.
[59] Schindelin, J., Arganda-Carreras, I., Frise, E., Kaynig, V., Longair, M., Pietzsch, T., Preibisch, S., Rueden, C., Saalfeld, S., Schmid, B., et al., 2012. Fiji: an open-source platform for biological-image analysis. Nat Methods 9, 676–682.

[60] Schlesinger, W.H., Klein, E.M., Vengosh, A., 2022. The global biogeochemical cycle of arsenic. Glob Biogeochem Cycles 36, e2022GB007515.
[61] Shaw, A.J., Szövényi, P., Shaw, B., 2011. Bryophyte diversity and evolution: windows into the early evolution of land plants. Am J Bot 98, 352–369.
[62] Shen, F., Qin, Y., Wang, R., Huang, X., Wang, Y., Gao, T., He, J., Zhou, Y., Jiao, Y., Wei, J., et al., 2023. Comparative genomics reveals a unique nitrogen-carbon balance system in Asteraceae. Nat Commun 14, 4334.
[63] Shi, S., Wang, T., Chen, Z., Tang, Z., Wu, Z., Salt, D.E., Chao, D.-Y., Zhao, F.-J., 2016. OsHAC1;1 and OsHAC1;2 function as arsenate reductases and regulate arsenic accumulation. Plant Physiol 172, 1708–1719.
[64] Song, W.Y., Park, J., Mendoza-Cózatl, D.G., Suter-Grotemeyer, M., Shima, D., Hörtensteiner, S., Geisler, M., Weder, B., Rea, P.A., Rentsch, D., et al., 2010. Arsenic tolerance in Arabidopsis is mediated by two ABCC-type phytochelatin transporters. Proc Natl Acad Sci USA 107, 21187–21192.
[65] Sun, D., Zhang, X., Yin, Z., Feng, H., Hu, C., Guo, N., Tang, Y., Qiu, R., Ma, L.Q., Cao, Y., 2023. As-hyperaccumulator Pteris vittata and non-hyperaccumulator Pteris ensiformis under low As-exposure: transcriptome analysis and implication for As hyperaccumulation. J Hazard Mater 458, 132034.
[66] Talavera, G., Castresana, J., 2007. Improvement of phylogenies after removing divergent and ambiguously aligned blocks from protein sequence alignments. Syst Biol 56, 564–577.
[67] Uraguchi, S., Sone, Y., Ohta, Y., Ohkama-Ohtsu, N., Hofmann, C., Hess, N., Nakamura, R., Takanezawa, Y., Clemens, S., Kiyono, M., 2018. Identification of c-terminal regions in arabidopsis thaliana phytochelatin synthase 1 specifically involved in activation by arsenite. Plant Cell Physiol 59, 500–509.
[68] Wang, C., Na, G., Bermejo, E.S., Chen, Y., Banks, J.A., Salt, D.E., Zhao, F.-J., 2018. Dissecting the components controlling root-to-shoot arsenic translocation in Arabidopsis thaliana. N Phytol 217, 206–218.
[69] Ware, A., Jones, D.H., Flis, P., Chrysanthou, E., Smith, K.E., Kümpers, B.M.C., Yant, L., Atkinson, J.A., Wells, D.M., Bhosale, R., et al., 2023. Loss of ancestral function in duckweed roots is accompanied by progressive anatomical reduction and a re-distribution of nutrient transporters. Curr Biol 33, 1795–1802 e4.
[70] Wysocki, R., Bobrowicz, P., Ułaszewski, S., 1997. The Saccharomyces cerevisiae ACR3 gene encodes a putative membrane protein involved in arsenite transport. J Biol Chem 272, 30061–30066.
[71] Xie, Q.E., Yan, X.L., Liao, X.Y., Li, X., 2009. The Arsenic Hyperaccumulator Fern Pteris vittata L. Environ Sci Technol 43, 8488–8495.
[72] Zhao, F.J., Wang, J.R., Barker, J.H.A., Schat, H., Bleeker, P.M., McGrath, S.P., 2003. The role of phytochelatins in arsenic tolerance in the hyperaccumulator *Pteris vittata*. N Phytol 159, 403–410.